ANL-6650

ANL-6650

Argonne National Laboratory

CRITICAL EXPERIMENTS ON THE JUGGERNAUT REACTOR

by

J. R. Folkrod and D. P. Moon

ANL-6650
Reactor Technology
(TID-4500, 18th Ed.)
AEC Research and
Development Report

ARGONNE NATIONAL LABORATORY
9700 South Cass Avenue
Argonne, Illinois

CRITICAL EXPERIMENTS ON THE JUGGERNAUT REACTOR

by

J. R. Folkrod and D. P. Moon

Reactor Engineering Division

December 1962

Operated by The University of Chicago
under
Contract W-31-109-eng-38
with the
U. S. Atomic Energy Commission

TABLE OF CONTENTS

LIST OF FIGURES

LIST OF TABLES

CRITICAL EXPERIMENTS ON THE JUGGERNAUT REACTOR

by

J. R. Folkrod and D. P. Moon

I. INTRODUCTION

The JUGGERNAUT is a light-water-cooled-and-moderated, graphite-reflected, heterogeneous thermal reactor located at Argonne National Laboratory. The reactor provides experimental facilities for the conduct of basic research in the range of neutron flux up to 4×10^{12} n/(cm^2)(sec) at an operating power of 250 kw.

The annular core of the JUGGERNAUT has a 46-cm (18-in.) internal diameter and a 61-cm (24-in.) outer diameter. Fully enriched uranium is contained in 240 plates positioned radially within 20 separate fuel assemblies. The fuel-bearing portion of plates is 57 cm ($22\frac{1}{2}$ in.) high and is reflected above and below by H_2O, which acts as both coolant and moderator. The radial reflectors are graphite. The neutron source consists of an antimony cylinder which is drawn up into a beryllium sleeve positioned on the reactor midplane, 30 cm (12 in.) from the outer core perimeter. The core and surrounding facilities are shown schematically in Figs. 1 and 2.

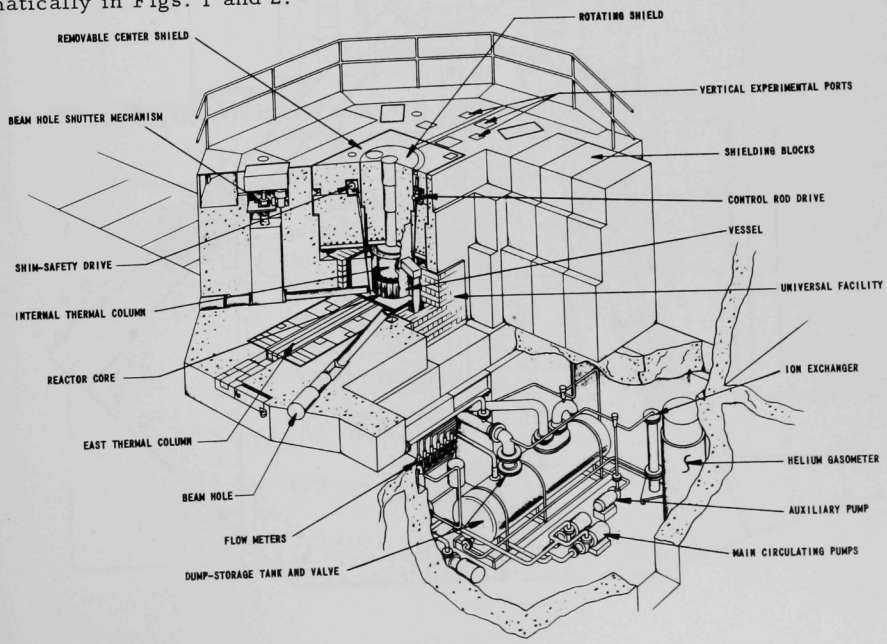

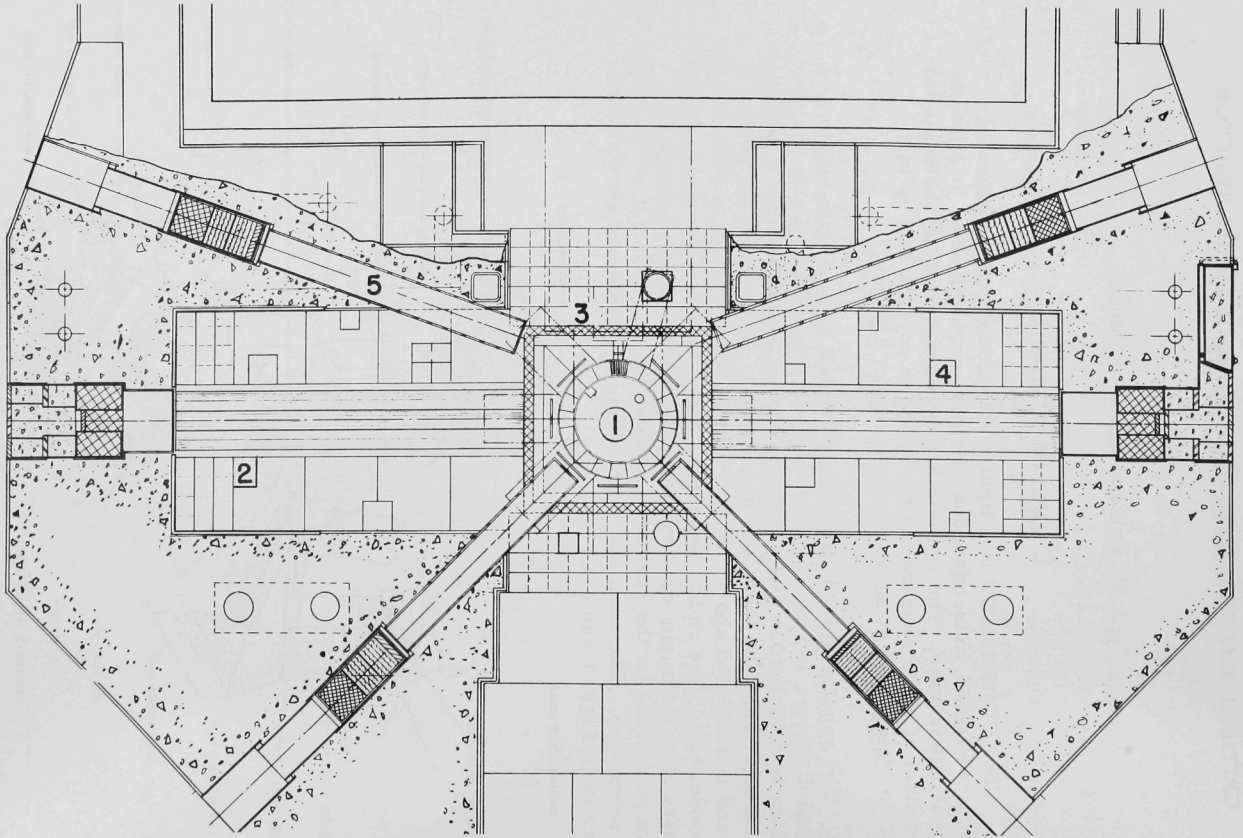

Fig. 2. JUGGERNAUT Section Showing Chamber Positions

Fuel was first loaded into the reactor on January 8, 1962, and criticality was obtained on January 11, 1962, with a fuel loading of 3.45 kg U^{235}. The experimental test program of the reactor was completed April 5, 1962, and confirmed that all safety criteria involving physics parameters were satisfied. Radiation surveys of the biological shielding and a power calibration at 250 kw were made. The temperatures of a fuel plate and a shim rod were observed during all power runs, and after shutdown, to verify that these components were maintained within safe temperature limits.

II. APPROACH TO CRITICAL

The initial fuel loading was prefaced by a rigorous performance test of all system components, instrumentation, safety interlocks, and alarms. The shim-safety rods and drive mechanisms were tested extensively to ensure smooth performance and a rapid insertion time (< 0.5 sec). The dump valve was tested repeatedly to ensure performance consistent with the specified complete drainage of the core in 4 sec.

The approach to critical was made with the use of five separate BF_3 counters and channels, from which inverse multiplication curves were obtained. The radial positions of the five BF_3 counters are shown in Fig. 2. The vertical positions are given in Table 1.

Table 1

VERTICAL POSITIONS OF BF_3 COUNTERS DURING APPROACH TO CRITICAL

Counter	Position (distance above core midplane)	Initial Counting Rate - No Fuel (cps)
1	75 cm ($29\frac{1}{2}$ in.)	100
2	60 cm ($23\frac{1}{2}$ in.)	48
3	60 cm ($23\frac{1}{2}$ in.)	30
4	100 cm ($39\frac{1}{2}$ in.)	56
5	0 cm	-

The counters were placed at the height indicated in order to obtain a counting rate of 100 cps or less with the source and moderator present, but no fuel. The maximum counting rate during the approach to critical was limited to 5000 cps. In order to stay within this limit, it was necessary to lower the source slightly after 3200 gm of U^{235} had been loaded into the core.

Each plate position in the core is identified by a fuel assembly number (1 through 20) and a plate number (1 through 12). The assemblies are numbered clockwise, starting with the first assembly to the east of the fine control rod. The plates are numbered clockwise within each assembly. Prior to loading any fuel into the reactor, each fuel assembly was assembled with dummy aluminum plates in positions 3 and 9, and fuel-bearing plates in all other positions.

Each fuel loading was made with the dump valve open and safety rods 1 and 3 raised. The water was then pumped up, after which the rods were raised in the following order: Shim No. 2, Safety No. 2, Safety No. 4, Shim No. 1, and Shim No. 3. Shim No. 2 was withdrawn before any of the other rods because it partially shielded the core from the source. The fine control rod was left in the "out" position during the whole approach to critical. The counting rate for each channel was determined after the water had been pumped up and after each rod withdrawal. These data were used to plot the inverse multiplication. After all rods had been withdrawn, the rods were scrammed and the multiplication determined again. Then, the water was dumped and a new fuel loading made.

The order in which the assemblies were loaded during the approach to critical is shown in Fig. 3. The initial loading was 1346.3 gm of U^{235}; this is approximately two-fifths the calculated critical loading and less than the minimum critical loading for the one-slab configuration in the ARGONAUT. The weights of U^{235} listed in Fig. 3 are ANL weights; the weights given by the manufacturer average 1% less than those given by ANL. The reactor was still slightly subcritical after all 20 fuel assemblies had been loaded, so it was necessary to remove a few assemblies and replace a limited number of dummy plates by fuel plates.

The inverse multiplication curves for Channels 1, 2, 3, and 4 are shown in Fig. 4. The extrapolated value of the critical mass is 3.40 kg, as indicated by each of the four channels. The critical loading was 3.455 kg, but the excess reactivity was 0.43% Δk. The assumption of a fuel worth of 0.0078% $\Delta k/gm$, as calculated, results in a critical mass of 3.40 kg. This is in exact agreement with that extrapolated from the inverse-multiplication curves. The critical mass in terms of the manufacturer's weights would be 3.36 kg. The inverse-multiplication curves with all shim-safeties inserted are shown in Fig. 5; the uncertainty is rather large, but a rough estimate of the total worth of the shim-safety system in terms of U^{235} can be taken as 1000 gm.

FUEL LOADING CODE		No 1
CORE POSITION	FUEL ASSEMBLY NUMBER	TOTAL U235 PER ASSEM.
1	6	184.7
2	7	169.0
3	4	168.3
4	11	168.8
5	9	184.2
6	12	168.8
7	17	168.4
8	1	168.5
9	8	183.6
10	2	166.2
11	3	166.6
12	13	170.1
13	18	184.6
14	10	170.0
15	5	167.1
16	14	169.4
17	20	185.4
18	16	169.2
19	19	167.5
20	15	169.1
TOTAL FUEL ASSEMBLIES		3454.5 grams
TOTAL U235		

LOADING NUMBER*	WEIGHT INCREMENT	TOTAL U^{235}
1	1346.3	1346.3
2	674.0	2020.3
3	336.3	2357.2
4	336.9	2693.5
5	169.4	2862.9
6	167.1	3030.0
7	170.0	3200.0
8	168.8	3368.8
9	85.7	3454.5

*ASSEMBLIES INSERTED AT EACH LOADING ARE INDICATED IN THE FIGURE.

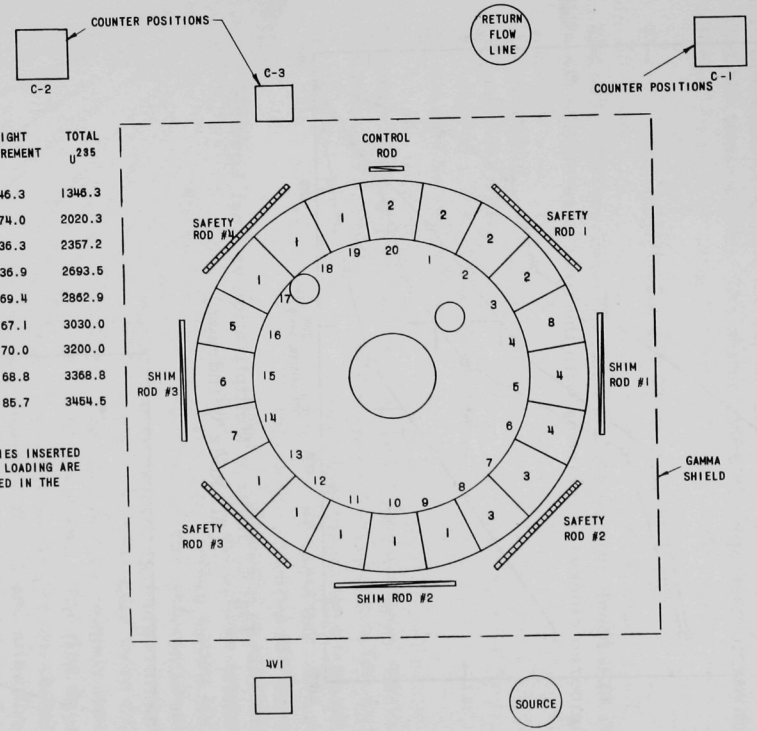

Fig. 3. Loading Chart for Approach to Critical

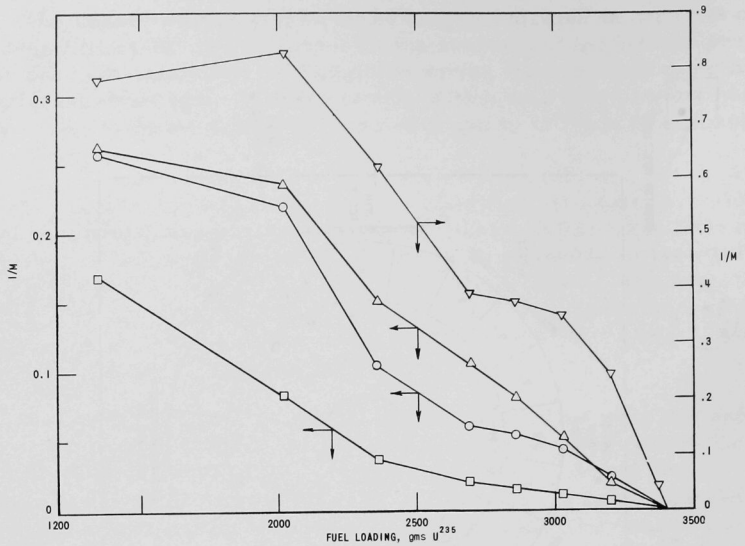

Fig. 4. Inverse Multiplication vs Fuel Loading (All Rods Withdrawn)

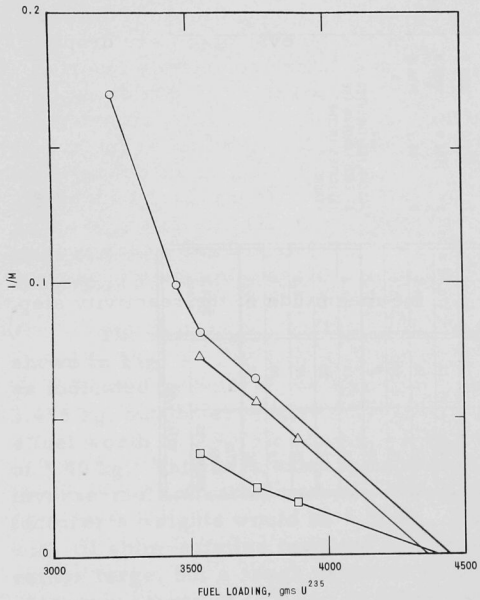

Fig. 5

Inverse Multiplication vs Fuel Loading (All Rods Inserted)

At no time during the approach to critical were the main pumps turned on. This precaution was taken because of the possibility that a change in the amount of water in the overflow line might affect the reactivity. For the same reason, the shield coolant pumps were not turned on.

III. CONTROL SYSTEM EVALUATION

The reactivity worth of the control system was determined by four different methods:

(1) rod drop;
(2) rod insertion;
(3) subcritical multiplication; and
(4) period measurement.

The rod drop method was used to obtain the individual worth of each of the rods and the worths of combinations of rods. In a few cases a rod calibration curve was also obtained by this method. The procedure used in the rod drop method was to achieve criticality at approximately 0.02 w with the source removed. Then, after having waited long enough for the delayed-neutron precursors to come into equilibrium, the rod or rods to be evaluated were dropped. The rods are completely inserted within 0.4 sec. The flux decay is followed on BF_3 or ion chamber channels for 75 sec after the rod drop. The worth of the rod is determined from pre-calculated curves (see Figs. 6, 7, and 8) which show the flux reduction for various times after the drop as a function of the magnitude of the reactivity step. This method has been compared with period calibration for rods in the ARGONAUT and found to agree within experimental error (3%).

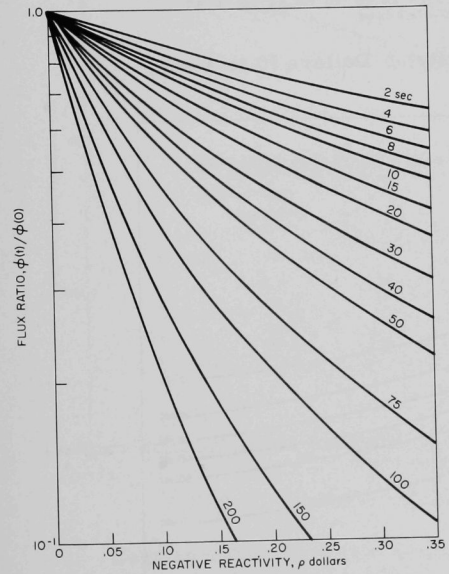

Fig. 6. Flux Ratio $\phi(t)/\phi(0)$ vs Negative Reactivity Step ρ Dollars at Time t sec After Step

Individual rod calibrations were also obtained by the rod insertion method. This method consists of achieving criticality and then inserting the rod to be calibrated at a slow and constant rate by the rod drive mechanism. The minimum driven

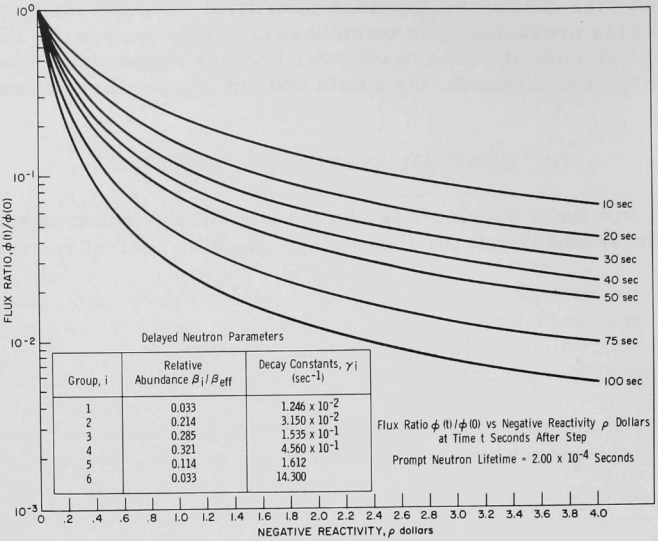

Fig. 7. Negative Reactivity, ρ Dollars (0 to 4 sec)

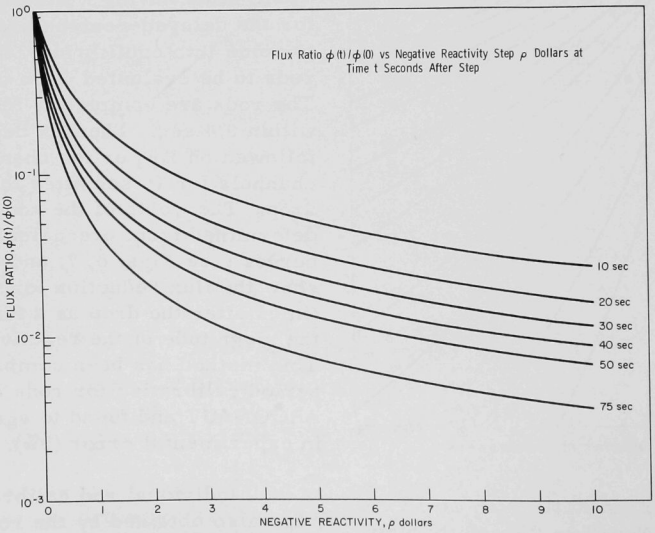

Fig. 8. Negative Reactivity, ρ Dollars (0 to 10 sec)

insertion time for each rod is 3 min. Even using this fastest drive-in speed, the accuracy of the calibration is poor for the last few inches of rod travel. The power trace from this experiment is used with code RE-138 on the IBM-704 to determine rod worth as a function of rod position.

The power signal was obtained from two BF_3 counters located on the core midplane in the east and west thermal columns far from the core (V2 and V7). In the calculation, the signal from each counter was weighted equally in order to correct for flux shifts caused by control rod movements. The signals from the BF_3 counters were fed into scalers which provided a record of the number of counts within a given time interval. This information was then recorded by an automatic printer.

The period method of reactivity measurement was used to calibrate the five control rods and to measure fuel worths and certain other small reactivity effects. The reactivity as a function of the positive asymptotic period is shown in Fig. 9.

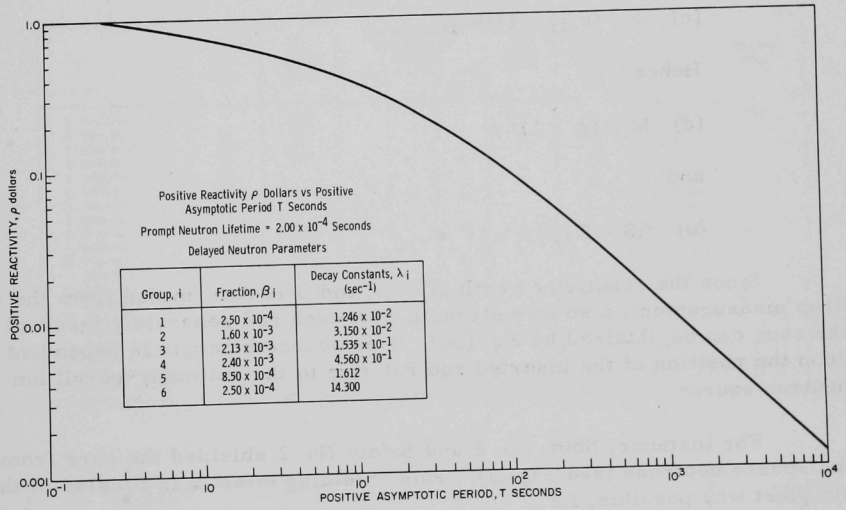

Fig. 9. Positive Asymptotic Period T Seconds

Certain difficulties are associated with the measurement of large rod worths by the rod drop method. Not only is it necessary to switch scales on the recorder after the drop, but changes in the flux shape may introduce error into the results. Hence, the total rod worths were also obtained by a subcritical multiplication technique. The following procedure was used.

(1) The worth of each rod is determined by the rod drop method.

(2) With the rod inserted, the source is brought into the reactor, and counting rates for the various channels are recorded after a constant power level is reached.

(3) The source strength S is determined from the data for each individual rod by the following equations:

(a) $M = C/f_iS$

$M \equiv$ neutron multiplication of the subcritical core

$C \equiv$ observed neutron counting rate

$f_iS \equiv$ neutron source strength

(b) $M = \frac{1}{1 - k_{eff}}$

$k_{eff} \equiv$ effective multiplication factor

(c) $\rho = (k_{eff} - 1)/k_{eff}$

Hence,

(d) $M = (\rho - 1)/\rho$

and

(e) $f_iS = C\rho/(\rho - 1)$.

Since the reactivity worth of each rod ρ is determined from the rod drop measurement, a source strength with each rod separately inserted in the core can be obtained by Eq. (3c). This source strength is dependent upon the position of the inserted rod relative to the antimony-beryllium neutron source.

For instance, Shim No. 2 and Safety No. 2 shielded the core from the source neutrons (see Fig. 3). This shielding effect was handled in the simplest way possible, i.e.,

$S \equiv$ true source strength

$f_iS \equiv$ apparent source strength with a particular rod i inserted

$f_i \equiv$ source shielding factor.

Then, for each shim-safety rod,

$M = C/f_iS$

and, with more than one rod inserted,

$$(f) \quad M = C/[\Sigma(1-f_i)]\, S \quad ,$$

assuming that the shielding effect of each rod is independent of any of the others. The "true" source strength was obtained by an averaging of the apparent source strengths measured for each of the rods excepting Shim No. 2 and Safety No. 2. The reactivity worth of a bank of rods is obtained from Eq. (3f) by observing the counting rate C with the rods inserted.

The rod worths obtained by the various methods are given in Tables 2 and 3. The effective delayed-neutron fraction was assumed equal to 0.0075. This value was obtained from a 3-group PDQ calculation in which all rods were assumed to be withdrawn. With shims rods inserted, the value of β_{eff} may be somewhat higher than 0.0075.

Table 2

ROD WORTHS (%Δk), 3454-gm LOADING

	Rod Drop Method	Rod Insertion Method	Subcritical Multiplication Method - Channel			Period Method	Evaluated from Fuel Worth	Best Value	Calculated Value
			1	2	3				
1. Fine Control	-	0.13	-	-	-	0.13	-	0.13	0.15
2. Shim No. 1	1.0	1.1	-	-	-	-	1.17	1.05	-
3. Shim No. 2	1.1	1.0	-	-	-	-	-	1.05	-
4. Shim No. 3	1.0	1.1	-	-	-	-	-	1.05	-
5. Safety No. 1	1.0		-	-	-	-	-	1.05	-
6. Safety No. 2	1.0		-	-	-	-	-	1.05	-
7. Safety No. 3	1.0		-	-	-	-	-	1.05	-
8. Safety No. 4	1.0		-	-	-	-	-	1.05	-
9. Shim No. 1 and Safety No. 2	1.8	-	2.0	-	2.0	-	-	1.9 ± 0.1	-
10. Shim No. 1 and Shim No. 2	1.9	-	2.3	-	2.3	-	-	2.1 ± 0.2	-
11. Shim No. 1 and Safety No. 3	2.1	-	2.3	-	2.3	-	-	2.2 ± 0.1	-
12. Shim No. 1 and Shim No. 3	2.1	-	2.3	-	2.4	-	-	2.2 ± 0.1	-
13. Shims 1, 2, 3	3.3	-	4.5	-	4.1	-	3.55	3.7 ± 0.4	3.5
14. Safeties 1, 2, 3, 4	4.3	-	4.6	-	5.0	-	-	4.6 ± 0.3	4.7
15. Shims and Safeties	7.5	-	7.7	5.5	9.5	-	7.2	7.5 ± 0.3	6.4

Reactor Condition: Runs 1 through 15, all rods banked except those tested, cold, clean, 3454-gm loading: k_{ex} = 0.43% Δk.

Table 3

ROD WORTHS (% Δ k)

Runs	With Shim No. 1 Inserted	Rod Drop Method	Rod Insertion Method	Runs	With Shim No. 1 Inserted	Rod Drop Method	Rod Insertion Method
16.	Safety No. 1	0.82	-	25.	Safety No. 1	0.93	0.9
17.	Safety No. 2	0.74	-	26.	Safety No. 2	0.57	0.7
18.	Shim No. 2	1.10	-	27.	Safety No. 3	0.56	0.7
19.	Safety No. 3	1.15	-	28.	Safety No. 4	0.93	-
20.	Shim No. 3	1.20	-	29.	Shim No. 1	-	0.95
21.	Safety No. 4	1.18	-	30.	Shim No. 2	-	0.85
22.	Total Seven-Rod Worth	7.7	-	31.	All Safeties	3.3%	-
23.	All Safeties	3.7	-	32.	Total Seven-Rod Worth	6.8%	-
24.	Total Seven-Rod Worth	7.3	-				

Reactor Condition: Runs 16-22, all rods withdrawn except Shim No. 1, cold, clean, 3539 gm loading, k_{ex} = 1.1% Δk.

Runs 23-24, safeties withdrawn, shims banked, cold, clean, 3739 gm loading, k_{ex} = 2.5% Δk.

Runs 25-28, 31, 32, safeties withdrawn, shims inserted, 3890 gm loading, beam tubes open, k_{ex} = 3.2% Δk.

Runs 29-30, Shim No. 1, 2 and Safety No. 4 withdrawn, Shim No. 3 inserted, other safeties banked at 7 in., 3890 gm, beam tubes open, k_{ex} = 3.2% Δk.

Calibration curves for the fine control rod and for the shims and safety rods are shown in Figs. 10 to 13 as obtained from both the rod drop method and the rod insertion method. These two methods complement one another. The largest error in the calibration by rod drop is for rod positions greater than 10 in., in which case the rod worth is the difference between two large numbers. The largest error in the calibration by rod insertion occurs for rod positions less than 10 in. because of the low intensity of the neutron flux when the rod reaches these positions.

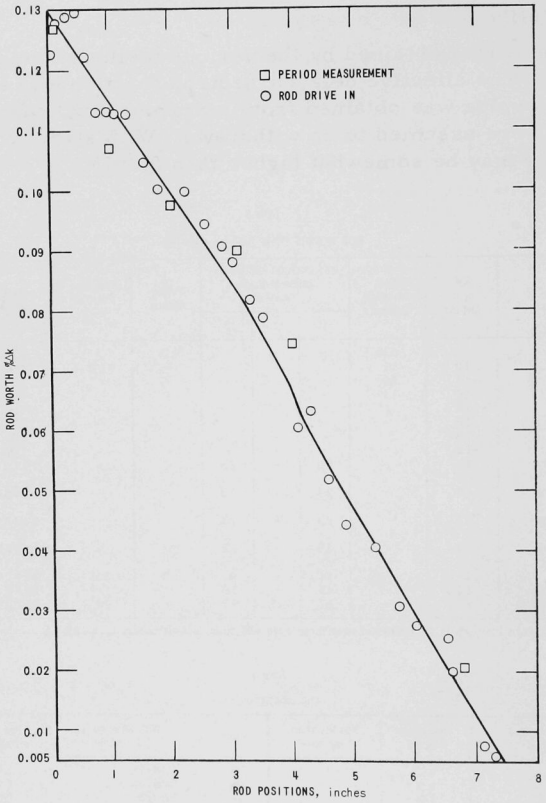

Fig. 10. Worth of Fine Control Rod

For the fully loaded core, with the beam tubes open, a consistent set of values for the worths of various rods is given in Table 4.

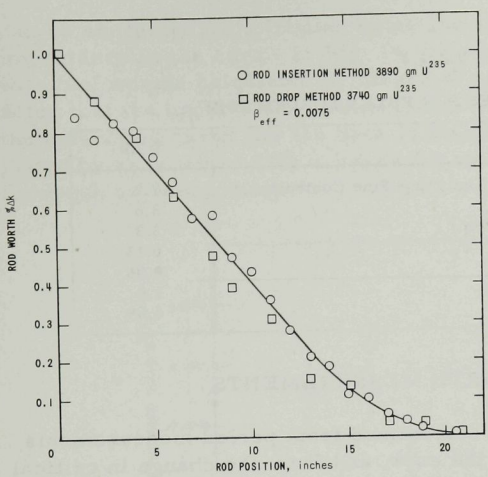

Fig. 11

Worth of Safety Rod
No. 1 or No. 4

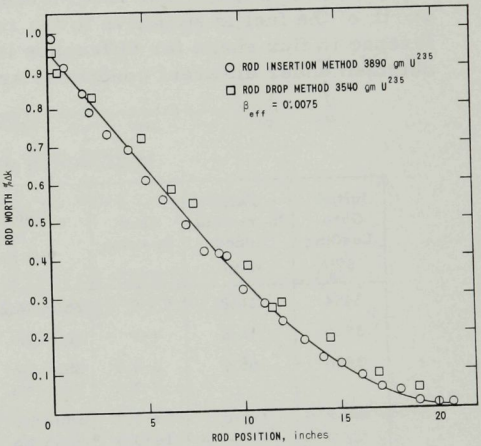

Fig. 12

Worth of Shim Rod No. 1

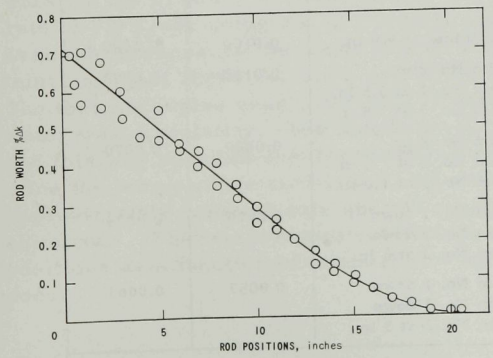

Fig. 13

Worth of Safety Rod
No. 2 or No. 3

Table 4

ROD WORTH VALUES FOR FULLY LOADED CORE

	% Δk
Total Control System Worth (including Fine Control)	7.0
Shim System Worth	3.6
Shutdown Margin (Safety System)	3.3
Fine Control Rod	0.13
Each Shim Rod	0.95
Safeties No. 1 and No. 4	1.0
Safeties No. 2 and No. 3	0.65

IV. FUEL WORTH MEASUREMENTS

The worth of the fuel was determined from period measurements after adding single fuel plates to the core, and from the change in critical rod positions when larger fuel increments were added. The indicated worth of the fuel is sensitive to the rod configuration because of the difference in flux shape for difference in rod configurations. The fuel worths obtained under different conditions are listed in Table 5. The values given

Table 5

FUEL WORTH MEASUREMENTS

Initial Core Loading (gm)	Fuel Increment Added (gm)	Core Position	Rod Positions (Rods up if not Mentioned)	Indicated Fuel Worth (%Δk/gm)	Corrected Fuel Worth (%Δk/gm)
3454	16.8	15-9	Shim No. 2 at 14.5 in.	0.0076	0.0076
3539	16.6	4-9	Shim No. 2 at 0.8 in.	0.0058	0.0058
3556	66.4	6-3,9 7-3,9	Shim No. 1 at 9.5 in. Shim No. 2 at 0.8 in.	0.0065	0.0078
3622	116.8	3-3,9 14-3,9 16-3,9 20-9	Shim No. 1 at 0 in. Shim No. 2 at 0.8 in. Shim No. 3 at 11.5 in.	0.0075	0.0065
3739	16.6	18-9	All Shims at 4.0 in.	0.0100	0.0080
3755	33.2	8-9 12-9	Shim No. 2 up Shim No. 1 at 3.5 in. Shim No. 3 at 3.5 in.	0.0112	0.0092
3789	34.0	2-9 10-9	Shim No. 2 up Shim No. 1 at 1.0 in. Shim No. 3 at 1.0 in.	0.0080	0.0070
3890	16.9	17-3	Shim No. 1 down Shim No. 3 down Shim No. 2 at 6 in.	0.0075	0.0075
3907	16.5	3-3	Shim No. 1 down Shim No. 3 down Shim No. 2 at 3 in.	0.0057	0.0063

can be corrected (to a limited extent) to correspond to a uniform angular importance in the core. In Fig. 14 these corrected values are compared with fuel worths calculated by means of perturbation theory. It is to be noted that the uncertainty in the measurements is rather large but that the calculated curve fits the data satisfactorily. The points have been adjusted by as much as 20% in cases for which the fuel was inserted at a flux peak or depression.

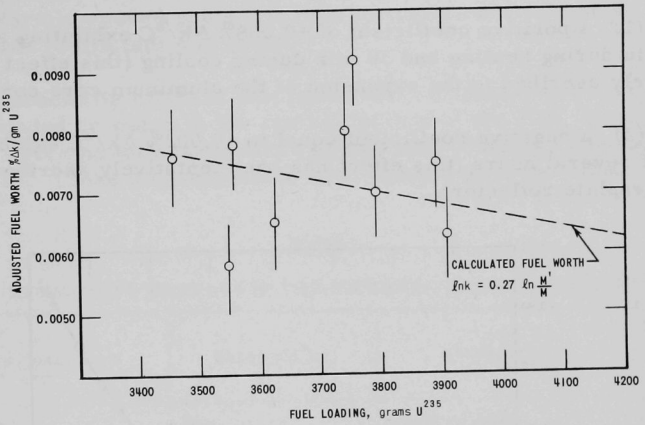

Fig. 14. Fuel Worth vs Fuel Loading

V. MEASUREMENT OF REACTIVITY COEFFICIENTS AND MISCELLANEOUS REACTIVITY EFFECTS

A. Temperature Coefficient

The core temperature coefficient was determined at a low reactor power by placing a 20-kw external heater in the flow system to heat the water in the primary system. Water was circulated through the core at a rate of 7.9 ℓ/sec using one of the main pumps. Three thermocouples were available to measure the water temperature. These were positioned in the inlet line, just above the core, and in the channel surrounding the weir. The thermocouples read within 2°C of one another throughout the tests when water was circulating. The maximum obtainable heating rate was 20°C/hr and this was possible only for temperatures below 60°C. In order to determine the temperature coefficient, the reactor was heated or cooled at an approximately constant rate and the reactor kept critical by adjusting the shim rods. The temperature coefficient was then deduced from the rod positions as a function of temperature and the calibration curves for the rods.

When the coolant water was heated under equilibrium conditions (5°C increase per hour), a constant negative temperature coefficient equal to -0.014% $\Delta k/°C$ was observed over the temperature range from 20°C to 80°C (see Fig. 15). When heated or cooled more rapidly (10 to 20°C per hour), a prompt temperature coefficient of reactivity equal to -0.020% $\Delta k/°C$ was observed. The difference between these values is attributed to a delayed positive temperature coefficient equal to +0.006% $\Delta k/°C$. The data indicate the existence of two contributions to this delayed coefficient:

(1) a positive coefficient of +0.008% $\Delta k/°C$ exhibiting a time delay of 90 min during heating and 30 min during cooling (this effect has been tentatively ascribed to the expansion of the aluminum core container); and

(2) a negative coefficient equal to -0.002% $\Delta k/°C$ exhibiting a time delay of several hours (this effect has been tentatively ascribed to heating of the graphite reflector).

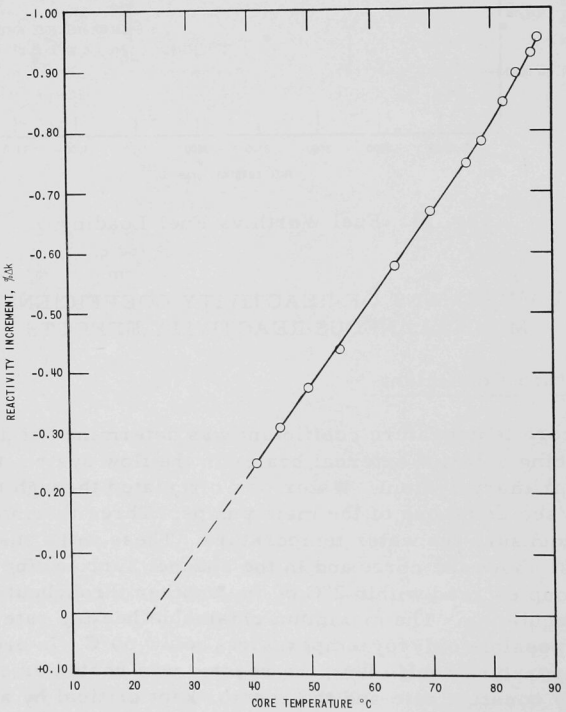

Fig. 15. Reactivity Increment vs Core Temperature

B. Void Coefficient

In order to simulate voids, Teflon plates (66 x 5.1 x 0.376 cm) were inserted between fuel plates in 15 of the 240 core positions, thus replacing 3.1% of the water in the active core. The measured void coefficient was -0.13% $\Delta k/1\%$ void, based on an active core water volume of 43 ℓ, and -0.16% $\Delta k/1\%$ void, based on a total water volume of 52 ℓ. A second measurement was made after 20% of the Teflon volume had been removed by drilling uniformly spaced holes (1.27 cm in diameter) in the plate. No change in void coefficient was noted.

The reactivity effect of the Teflon was compared with that of air when surrounded by water in the central facility of the ITC. Within experimental error no difference could be detected between Teflon and air (see Table 6). These measurements were made with a core loading of 3739 gm U^{235}.

Table 6

REACTIVITY EFFECTS IN THE INTERNAL THERMAL COLUMN

Material Removed	Replaced By	Configuration	Reactivity Effect (%Δk)
1. Graphite	Air	Total volume	-1.1
2. Air	Teflon (2200 cc)	Cylinder (66 cm high)	+0.35
3. Air	U^{235} (16.6 g)	Fuel plate	+0.33
4. Air	Steel	Pipe (60 cm high x 11.3 cm OD x 10 cm ID)	-1.6
5. Air	Cadmium (503 cm^2)	Plate (60 cm high)	-2.2
6. Air	Water	Total volume	-4.2
7. Water	Steel	Pipe (60 cm high x 11.3 cm OD x 10 cm ID)	-1.6
8. Water within steel pipe	Air	Cylinder (66 cm high)	+2.0
9. Water within steel pipe	Teflon (2200 cc) and air	Cylinder (66 cm high)	+2.0

C. Effect of Overflow Line

Because it was thought that a change in water flow through the return flow line (see Fig. 3) might have a small but observable effect on reactivity, care was taken to keep the flow constant throughout the approach to critical. After criticality had been achieved, the reactivity effect of the coolant flow rate was tested by varying the opening of the throttle valve to achieve flows from 0.2 ℓ/sec to 8 ℓ/sec. No change in reactivity was observed.

D. Effect of Shield Coolant Line

The worth of water relative to void in the coolant lines of the lead thermal shields was measured to be -0.045% Δk. Turning off the shield coolant pumps when the reactor is critical resulted in a positive period of 170 sec.

E. Worths of Top Reflector and Core Moderator

The worth of the water moderator and reflector was measured by means of the same instrumentation as was used to determine rod worths by the insertion method. A critical condition was achieved at a low power, after which the water was drained slowly into the dump-storage tank by way of the primary inlet flow line. Previous to the experiment, it was necessary to remove the disc from the check valve which normally prevents return flow to the dump storage tank.

The water level was reduced at a rate of approximately 0.5 cm/sec; total water removal was accomplished in 2 min. It was necessary to bypass the overflow and low-flow interlocks so that the control rods would not scram during the experiment. A worth of 0.5% Δk was obtained for the top reflector, and a worth of approximately 20% for the core water (see Fig. 16). This latter figure may well be in error (an underestimate) since

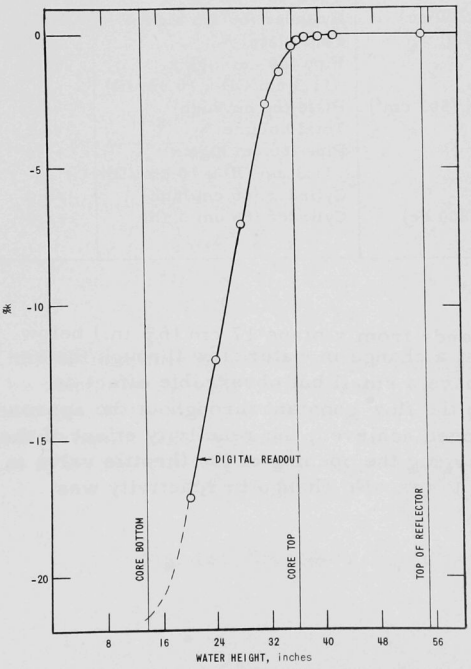

Fig. 16

Reactivity Change as a Function of Water Height

the leakage characteristics of the core would change significantly as the water is lowered. This measurement was made with a core loading of 3739 gm U^{235}.

F. Worth of Beam-tubes Graphite

The reactivity effect of voided beam tubes (see Fig. 2) compared with beam tubes filled with 2 ft of graphite was determined by moving a previously calibrated shim rod to maintain criticality, while removing the graphite from one beam hole at a time. The reactivity effects of the voided beam tubes relative to graphite-filled tubes measured to be as follows:

Beam Tube No.	Δk
1	-0.026
2	-0.264
3	-0.325
4	-0.010

Theoretically, the reactivity effects of tubes Nos. 1 and 4 should be equal, as should the reactivity effects of tubes Nos. 2 and 3. The observed differences probably result from a flux asymmetry caused by a nonuniform rod insertion pattern. These measurements were made with a core loading of 3539 gm.

G. Perturbation Experiments in ITC

The reactivity effects associated with inserting various materials in the central graphite facility of the ITC were determined from critical control rod positions, and, in certain cases when criticality could not be obtained, by subcritical multiplication measurements.

When the central graphite plug is removed from the ITC, an aluminum-lined void region, 15 cm (6 in.) in diameter by 120 cm (47 in.) deep, is created. This region extends from a plane 17 cm ($6\frac{3}{4}$ in.) below the core to a plane 47 cm ($18\frac{1}{2}$ in.) above the core. When plates of Teflon, steel, cadmium, or fuel were inserted in this region, they were supported by means of a solid graphite block which had its top surface level with the plane defined by the bottom edge of the core fuel plates. This support was present during all the experiments in the ITC. The reactivity effects measured are listed in Table 6.

VI. FLUX MEASUREMENTS

Prior to the operation of the reactor at full power, critical runs were made at low power to measure flux levels. Absolute thermal-neutron flux measurements were obtained by a cadmium difference technique using 1-cm^2 x 0.00254-cm-thick gold foils calibrated in the Argonne Standard Pile. Eight separate runs were made to obtain relative flux values in the various experimental facilities for both symmetric and asymmetric settings of the control rods. The data from these experiments were normalized by use of a gold foil at the center of the internal thermal column. Calculations have shown that the flux per unit core power at this position will be constant to within 5% no matter how the control rods are arranged.

The maximum thermal-neutron fluxes obtainable in the various experimental facilities are listed in Table 7. The thermal-neutron fluxes within beam tubes are shown in Fig. 17. The thermal fluxes and cadmium ratios in the horizontal thermal columns are shown in Figs. 18 and 19, respectively. The asymmetric rod pattern mentioned on Fig. 18 was obtained by inserting Safeties Nos. 1 and 2 and Shim No. 1, withdrawing Safeties Nos. 3 and 4 and Shim No. 3, and leaving Shim No. 2 halfway inserted.

Table 7

THERMAL-NEUTRON FLUX IN EXPERIMENTAL FACILITIES
AT A REACTOR POWER OF 250 kwt

Experimental Facilities*	Thermal Flux [$n/(cm^2)(sec)$ maximum except where specified]	Cadmium Ratio (gold foils)
Core	1.5×10^{12} (average) 2.5×10^{12}	2.35
Internal Thermal Column (ITC)	3.8×10^{12}	3.58
Test Cave	2.0×10^{11} 1.0×10^{11} (average)	10.4
Universal Facility	1.6×10^{11} 0.8×10^{11} (average)	15.1
Thermal Columns	1.0×10^{12}	3.70
Vertical Facilities		
V1	1.4×10^{9}	134
V2	6.6×10^{9}	2118
V3	8.7×10^{9}	18.3
V4	4.9×10^{11}	17.4
V5	1.7×10^{10}	11.8
V6	7.1×10^{11}	4.36
V7	1.4×10^{10}	88.3
V8	5.5×10^{11}	49.7
V9	6.4×10^{10}	125
V10	7.0×10^{9}	834
V11	2.4×10^{11}	9.88

*See Figs. 1 and 2 for identification of facilities.

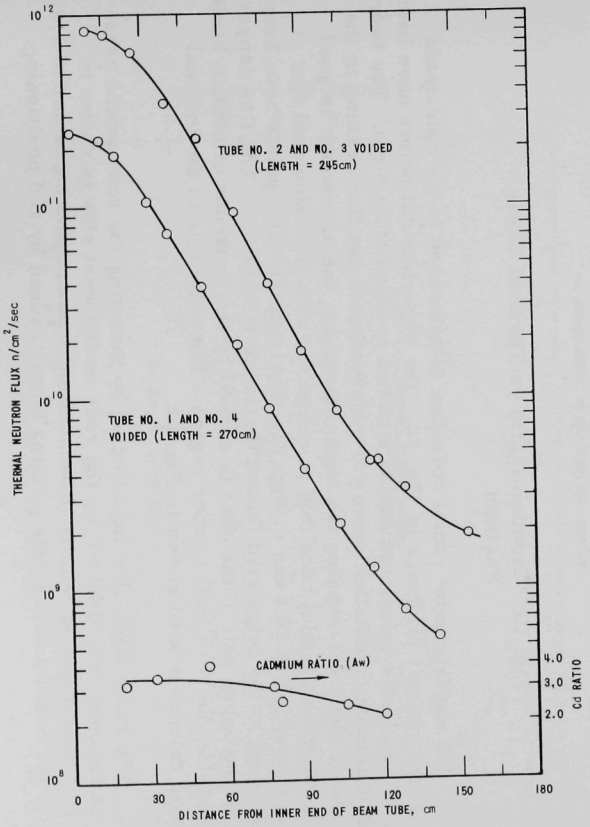

Fig. 17. Thermal-neutron Flux vs Beam Tube Position

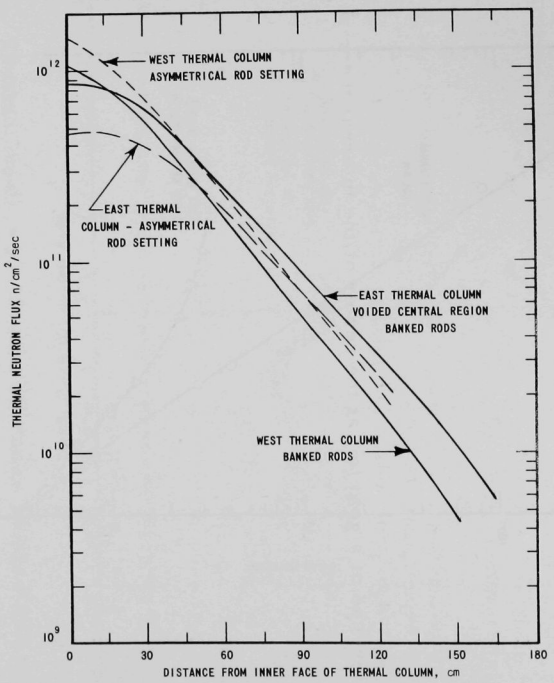

Fig. 18. Thermal-neutron Flux vs Thermal Column Position

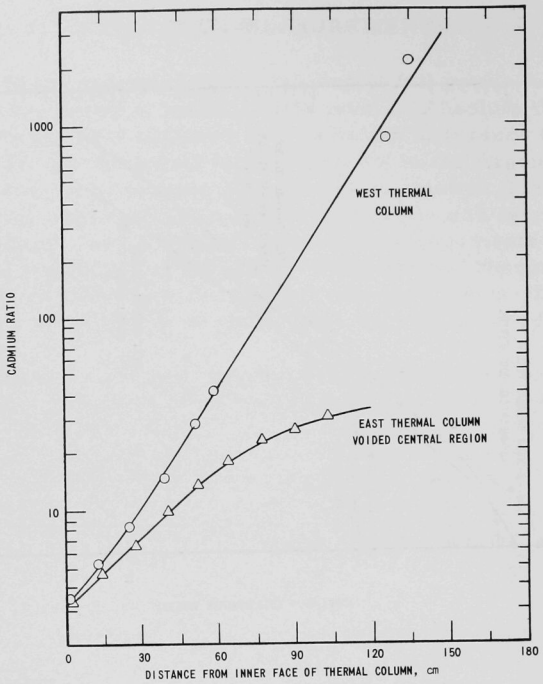

Fig. 19. Cadmium Ratio vs Thermal Column Position

The experimental radial core flux is compared to the calculated flux at the reactor midplane in Fig. 20. The experimental points have been normalized to the calculated flux at a radial position of 23.5 cm. The two-group diffusion calculation seems to underestimate the flux peaking in the thin water shell surrounding the core; otherwise, the agreement is good. The experimental axial core flux is compared with the calculated flux at a radial position of 26.6 cm in Fig. 21. The experimental points have been normalized to the calculated flux at the reactor midplane. The flux depression in the upper half of the core is caused by the presence of control blades just outside the core in the upper region. The axial flux in the internal thermal column is also shown in Fig. 21.

The radial-flux skewing effected by inserting the rods on the east side of the core and withdrawing the rods on the west side is shown in Fig. 22. This skewing results in an additional power peaking factor of 1.4. This is the maximum possible peaking factor caused by rod positioning.

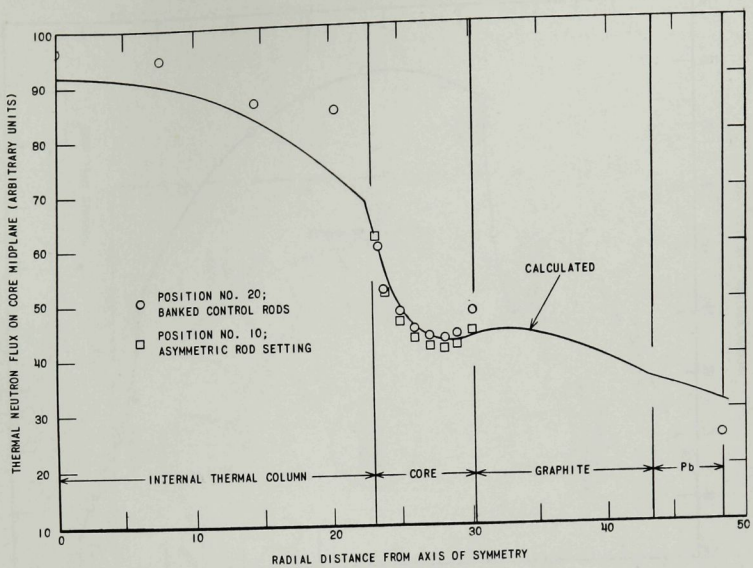

Fig. 20. Thermal-neutron Flux as a Function of Radial Position at Core Midplane

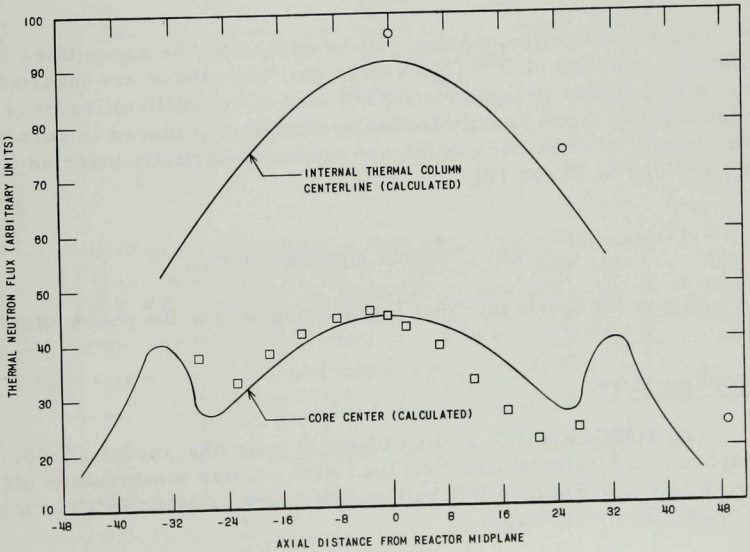

Fig. 21. Thermal-neutron Flux as a Function of Axial Position for Core and Internal Thermal Column

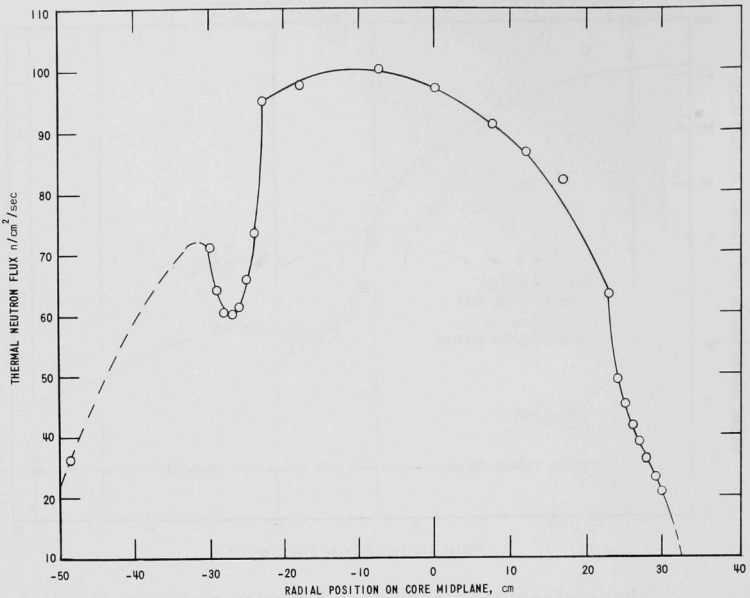

Fig. 22. Thermal Flux Pattern Caused by Asymmetrical Rod Positioning

Additional power peaking will be caused by the assemblies containing heavier loadings of U^{235} (240 vs 202 gm) when these are inserted in the core. Although this peaking should not lead to any difficulties, it is recommended that the more heavily loaded assemblies be placed in core positions in the vicinity of shim rods which are normally partially inserted (i.e., core positions 5, 15, or 10).

VII. POWER EXPERIMENTS

Figure 23 shows the final fuel loading before the power tests were made.

A. Cooling Tower

The JUGGERNAUT cooling tower is a Brinks' model 4B-40. It has the capacity to dissipate a 250-kw load with a water temperature off the tower at 32°C (90°F) and a wet bulb temperature of 24°C (75°F) at a maximum water flow of 100 gpm.

FUEL LOADING CODE			FINAL No LOADING
CORE POSITION	FUEL ASSEMBLY NUMBER	TOTAL U235 PER ASSEM.	
1	6	202.3	
2	7	202.5	
3	4	201.6	
4	11	202.2	
5	9	200.8	
6	12	201.8	
7	17	201.8	
8	1	201.6	
9	8	204.7	
10	2	201.1	
11	3	200.6	
12	13	203.7	
13	18	201.6	
14	10	203.2	
15	5	200.7	
16	14	203.0	
17	20	202.3	
18	16	202.4	
19	19	201.2	
20	15	202.5	
TOTAL FUEL ASSEMBLIES	20	4041.5 grams	
TOTAL U235			

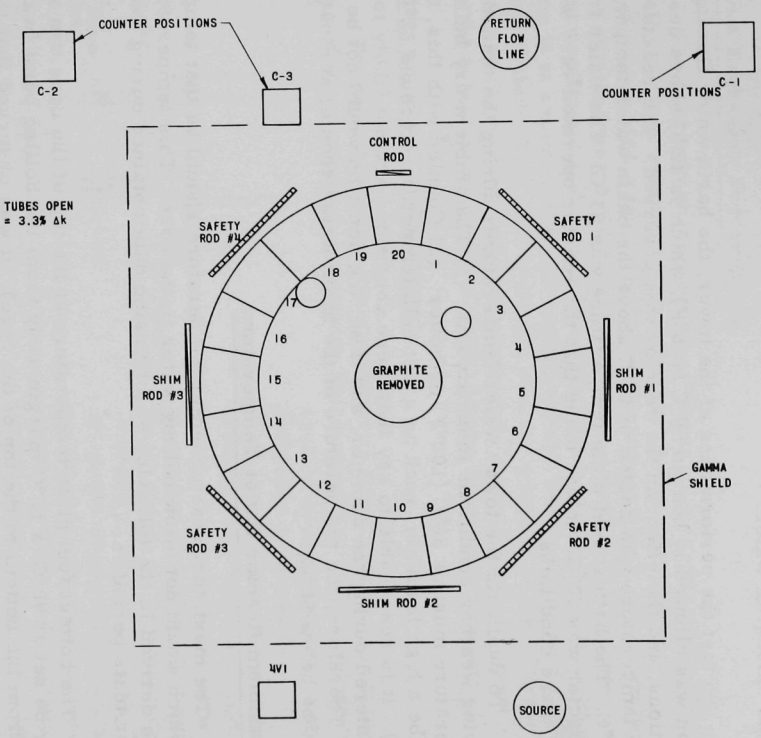

Fig. 23. Final Core Loading

A thermocouple wire was temporarily put in the tower basin water, and the water flow to and from the tower was determined by timing a weighed amount of water.

To test the performance of the tower, the basin water flowing at 85 gpm was allowed to heat to 50°C (106°F), which is 12°C above design conditions, and the effect on the reactor was observed. The reactor inlet water temperature was heated to 15°C above the basin water temperature, or 65°C. The hottest fuel plate temperature was 83°C. The water from the reactor was 72°C. It was found that the reactor operated very well under these conditions.

To duplicate the tower water temperatures during the test, the following weather conditions must prevail. (1) The ambient dry bulb temperature must be 38°C (100°F) or hotter. (2) Coupled with this, there must be a high humidity, such as a wet bulb temperature around 32°C (90°F). It is reasonable to say that these conditions are not likely to be encountered during the summer, and if so, the duration would not be for long. Therefore, the temperature of the basin water should, at most times, be below 50°C.

B. Maximum Reactor Outlet Temperature

The maximum reactor outlet temperature should be that temperature which would not allow boiling water in the core. This temperature may be derived in the following way by using data obtained during the reactor tests period.

The hottest fuel plate temperature at the top of the core can arbitrarily be set at 90°C, a 10°C margin away from the boiling point (water flows from the bottom to the top of the core). It was observed that the plate temperature was about 11°C hotter than the bulk water temperatures along its length (see Table 8). Therefore, the maximum outlet water temperature at the top of the core is 90°C - 11°C or 79°C.

Table 8

MAXIMUM FUEL PLATE TEMPERATURES WITH VARIOUS WATER TEMPERATURES
Heat Exchanger U_{avg} = 2.8 kw/(m²)(°C)

Basin Temperature, °C	Reactor Outlet Temperature, °C	Maximum Fuel Plate Temperature, °C
20	46	56
32	57	66
36	61	72
38	65	75
50	72	

Table 8 correlates the tower basin water, reactor outlet water, and maximum fuel plate temperature.

C. Heat Exchanger Performance

The heat exchanger used is a "Young" single-pass SSF-606-ER-1P. It is all stainless steel with $\frac{3}{8}$-in.-diameter tubes giving a total heat transfer area of 5.25 m^2 (56.4 ft^2). The highest average overall heat transfer coefficient obtained was 2.8 kw/(m^2)(°C) [495 Btu/(hr)(ft^2)(°F)]. This is an excellent coefficient and is indicative of clean tubes in the heat exchanger. In time it is expected that the coefficient will become less as the tubes become fouled. This will cause the reactor water to become hotter in relation to the coolant, and if encountered, it may be advantageous to clean the tubes of the heat exchanger before the summer months.

D. Reactor Power Measurement

Temperature of the reactor water is taken at three positions by means of three chromel-constantan thermocouples. This material was used because it generates about 20% more millivolts per °C (0.06 mv/°C) than the next highest thermocouple material. Since small ΔT's were to be measured, it was believed that the driving force should be as large as possible in order to reduce errors. The inlet water temperature (T_3) was measured in the pipe one meter below the bottom of the vessel. The second thermocouple (T_2) is above the core in the annulus. The third couple (T_1) is in the trough in front of the return line opening to measure the mixed water temperature (see Fig. 24).

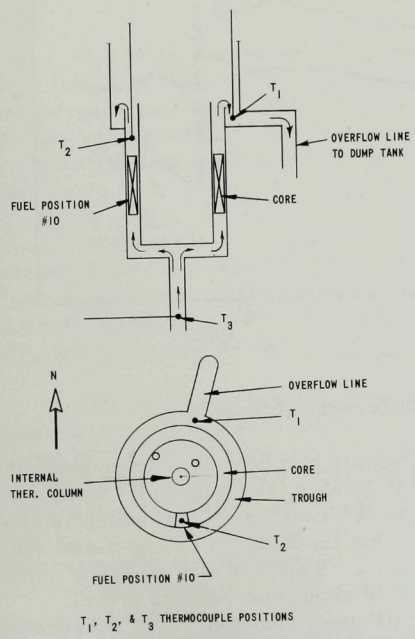

Fig. 24. Reactor Thermocouple Positions

Gold and uranium foils were used to determine the power output (watts) of the core at low level. This information was extrapolated to 250 kw. As the power of the reactor was increased to produce readable ΔT's, it was found that the power, calculated from the observed temperatures and flow, did not agree with that predicted from foils. The calculated power was low by about a factor of 2 at the 250-kw level than predicted by the foil measurements.

To check the core ΔT, two iron-constantan thermocouples were installed in the heat exchanger on the primary side. These were read-out on a separate potentiometer. The ΔT obtained gave a power output greater than the desired 250 kw. The power dissipated at the cooling tower was also checked, and the result agreed with the primary output at the heat exchanger.

Figure 25 shows the core ΔT's during the 24-hr power run. Curve T_2T_3 depicts the ΔT across a specific portion of the core (fuel position 10). Curve T_1T_3 gives the average ΔT for the core because T_1 is in the trough where all the reactor water passes and is well mixed. There is a difference between the ΔT's of about 0.3°C, which is equivalent to 10 kw. Since T_1 is down stream from T_2 (T_1T_2 = 0.3°C), this indicated one of two things. The 10 kw of heat was given off somewhere in the reactor structure, or the volume of the core at T_2 was producing heat above the average.

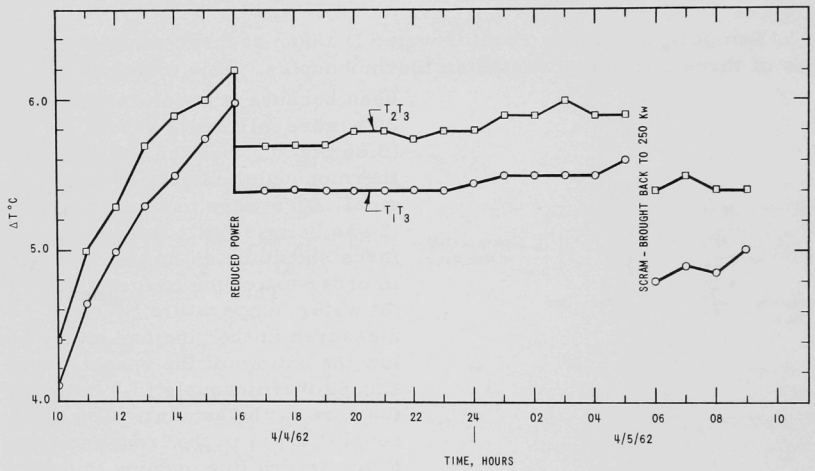

Fig. 25. Temperature Difference Across Core

Transferring this heat to the graphite can be ruled out because it operates at a higher temperature than the water (see Fig. 26). Sufficient surface area to transfer 10 kw of heat to the reactor shield, which is at a lower temperature, is not available, so this mechanism can be ruled out. Thermocouple T_2 is next to Shim Rod No. 2. This rod was used for shimming and it was withdrawn 10 in., which is about one-half its travel. Shim Rods Nos. 1 and 3 were in their full-down position. It is reasonable to expect that the volume of the core at Shim Rod No. 2 was producing power above the average for the core because of the high flux due to withdrawing Shim Rod No. 2. This can account for the larger ΔT shown by Curve T_2T_3.

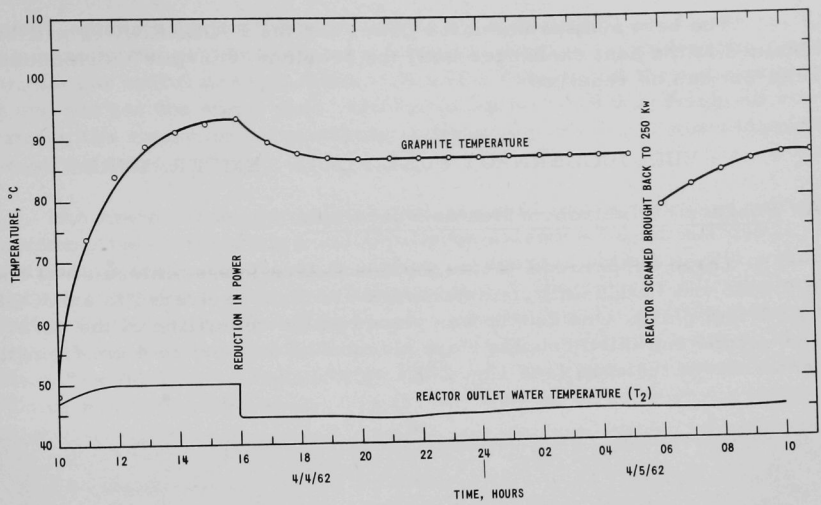

Fig. 26. Graphite Temperatures

Figure 25 shows that T_1T_3 and T_2T_3 increased in value between 10:00 and 16:00 hours. During this time the ΔT across the heat exchanger was constant and was higher than the core ΔT, which indicated that the reactor was operating at a higher level than desired. At this time, the secondary system was checked for power output at the cooling tower. At 1600 hours, a 20% reduction of power was made. There were immediate decreases of T_1T_3 and T_2T_3 to 5.4°C and 5.7°C, respectively, and those values remained constant until 2300 hours. Then a slight rise was experienced until the reactor was inadvertently scrammed at 0500 hr. The reactor was taken to power at 0600 hr. Shim rod No. 2 was at 14 in. which accounts for the greater ΔT between T_1T_3 and T_2T_3; however, T_1T_3 and T_2T_3 had lower values, which cannot be explained at present.

The ΔT at the heat exchanger reduced 20% when the reduction of power was made and was constant; the data were always reproducible. Values of T_1T_3 and T_2T_3 should read between 7°C and 8°C. Temperature T_3 (that at the inlet to the reactor) agrees very closely with the outlet temperature of the heat exchanger, but T_1 and T_2 were always 2°C or 3°C less than the inlet temperature of the heat exchanger. There is no good explanation for the behavior of T_1 and T_2. Perhaps there is an error introduced due to neutron and/or gamma flux. A copper-constantan thermocouple was placed alongside T_2 for a check. Initially, it read 3°C above T_2. After 24 hr in the reactor the reading was 1°C below T_2. This thermocouple had very little reactor operating time, so this change may not be a function of integrated neutron flux but due to the gamma flux received during the 24 hr in the reactor.

The best measurement for power for the JUGGERNAUT will be obtained at the heat exchanger until the problem of in-pile thermocouple read-out can be resolved.

VIII. JUGGERNAUT FUEL PLATE TEMPERATURES

A. Position of Thermocouples on Fuel Plate

Three copper-constantan thermocouples in a stainless steel sheath of 0.0635-cm (0.025-in.) diameter were aluminum soldered to a JUGGERNAUT fuel plate. One couple was placed at the centerline of the core. The second and third couples were placed 12.7 cm and 25.4 cm from the centerline of the core (see Fig. 27).

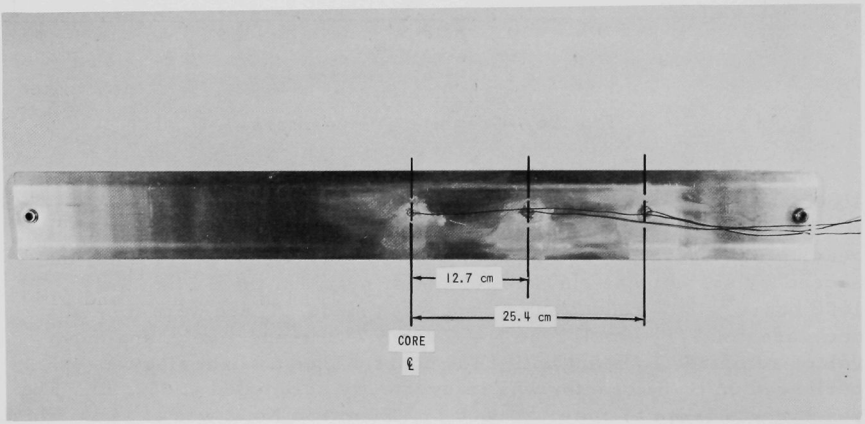

Fig. 27. Position of Thermocouples on Fuel Plate

B. Operating Temperatures of Fuel Plate at Full Power (250 kwt)

The fuel plate operates about 11°C hotter than the bulk water temperature. This ΔT is equal along the plate where the temperatures were measured. In order not to boil the water, the outlet water temperature should be kept below 77°C.

C. Temperature of the Fuel Plate after Water Dump at Full Power (250 kwt)

The JUGGERNAUT reactor has a water-dump system which is a shutdown safety device. The water may be dumped at the operating power level by pushing the total scram button which also drops the control rods.

The heat, which is generated after shutdown, is carried away by the helium atmosphere to the cooler areas of the reactor system. With an open dump valve, the gas will flow from dump tank to the bottom and through the hot core and back to the dump tank. The following test was performed to determine the maximum temperature of the fuel plate which was representative of the core.

The reactor was operated 24 hr to build in fission products and to determine plate temperatures subsequent to a water dump at full power. This finite operating time gave five-eighths of the heat which would be released after infinite operation or two-thirds of the heat produced after operation for a month. The dump valve was closed seconds after the dump scram to reduce convective helium currents. This gave the most severe condition for the test. The maximum fuel plate temperature obtained was 100°C one hour after shutdown. The three thermocouples gave the same readings.

The dump valve would not be closed after a water dump scram in normal operation. Therefore, the core should not get as hot as indicated by the test because the cooling action of the helium would become more effective. The hazards report(1) states that with the dump valve open the fuel temperature would reach 192°C after infinite operation. Assumptions were made for this particular case that the gamma and beta energy was absorbed in the fuel and that the helium temperature was at 93°C. This was not the actual case for only one-half of the total energy was absorbed in the fuel, mainly the beta. Also, the helium temperature was 65°C. Considering these facts, calculations show that for 24-hr operation and with the dump valve open, the temperature of the fuel would be 95°C, and, after an infinite operation, ~110°C.

IX. SHIM AND FINE CONTROL ROD TEMPERATURES

An iron-constantan thermocouple in a stainless steel sheath of 0.0635-cm (0.025-in.) diameter was placed in contact with Shim Rod No. 1 and the fine control rod. The couples were placed at the midplane of the core.

The maximum shim rod temperature was 160°C and the fine control rod temperature was 105°C while the reactor was operating at 250 kwt.

---

(1)J. R. Folkrod et al., Hazards Summary Report on the JUGGERNAUT Reactor, ANL-6192, (Feb 1961) p. 59.

X. GRAPHITE TEMPERATURE

A chromel-constantan thermocouple was buried in the reflector graphite. The location was 5 cm from the vessel wall directly beneath 6H2 beam hole, which opens at the southeast face of the reactor.

Figure 26 shows the temperature of the graphite during the 24-hr operation. It appears that the graphite would level off at 94°C if a reduction of reactor power was not made at 1600 hr. Three hours after the power reduction the graphite equilibrium temperature was 87°C. The temperature reduced to about 75°C after the accidental scram at 0500 hr. The reactor was brought to full power at about 0530 hr and in 4 hr the graphite reached equilibrium condition of 87°C.